



Published in final edited form as:

Traffic. 2008 September ; 9(9): 1551–1562. doi:10.1111/j.1600-0854.2008.00786.x.

Identification of Acidic Dileucine Signals in LRP9 that Interact with Both GGAs and AP-1/AP-2

Balraj Doray^{1,†}, Jane M. Knisely^{2,†}, Lukas Wartman¹, Guojun Bu², and Stuart Kornfeld^{1,*}

¹Department of Internal Medicine, Washington University School of Medicine in St.Louis, St. Louis, MO 63110

²Department of Pediatrics, Washington University School of Medicine in St.Louis, St. Louis, MO 63110

Abstract

The GGA family of monomeric clathrin adaptors are known to bind to cargo molecules via short C-terminal peptide motifs conforming to the sequence DXXLL (X= any amino acid), while the heterotetrameric adaptors AP-1 and AP-2 utilize a similar but discrete sorting motif of the sequence [D,E]XXXL[L,I]. While it has been established that a single cargo molecule may contain either or both types of these acidic cluster-dileucine (AC-LL) sorting signals, there are no examples of cargo with overlapping GGA and AP-1/AP-2 binding motifs. Here we report that the cytosolic tail of LRP9 contains a bifunctional GGA and AP-1/AP-2 binding motif at its carboxy terminus (EDEPLL). We further demonstrate that the internal EDEVLL sequence of LRP9 also binds to GGAs in addition to AP-2. Either AC-LL motif of LRP9 is functional in endocytosis. These findings represent the first study characterizing the trafficking of LRP9 and also have implications for the identification of additional GGA cargo molecules.

Keywords

GGAs; AP-1; AP-2; dileucine motif; endocytosis; LRP9

Introduction

The intracellular trafficking of membrane proteins, including receptors and transporters, is dependent upon short peptide sorting motifs present in the cytoplasmic tails of these proteins (1). These sorting motifs are recognized by adaptor proteins that collect and package the membrane proteins into transport carriers for delivery to the target compartments. Prominent among the adaptor proteins are the heterotetrameric clathrin adaptors AP-1 and AP-2, and the monomeric clathrin adaptors termed GGAs (Golgi-localized, γ -ear containing ARF-binding proteins). AP-1 and AP-2 bind YXX ϕ (ϕ -bulky hydrophobic) motifs via their μ subunits and [D,E]XXXL[L,I] motifs via their $\gamma/\sigma 1$ (for AP-1) and $\mu/\sigma 2$ (for AP-2) hemicomplexes (1). The GGAs, by contrast, bind DXXLL sequences. In the examples described to date, the DXXLL motifs have been situated one or two residues from the carboxy terminus of the cargo protein. This location has been shown to be critical for binding to the GGAs since the addition of a few alanines to the carboxyl end of the cargo molecules blocks interactions with these adaptors (2,3).

* Corresponding author: Stuart Kornfeld; skornfel@im.wustl.edu.

† These authors contributed equally to this work.

With the exception of low density lipoprotein receptor (LDLR)-related protein 3 (LRP3) and BACE, DXXLL motifs found in receptors that interact with the GGAs do not overlap with [D,E]XXXL[L,I] motifs that bind to AP-1 and AP-2 (1). Even in the case of LRP3 and BACE, it is not known if these same motifs are bifunctional.

LRP3, along with its related family members LRP9 (4) and LRP12 (5), contains a C-terminal acidic cluster dileucine (AC-LL) signal conforming to both the consensus GGA-binding DXXLL motif and AP-1/AP-2-binding [D,E]XXXL[L,I] motifs (1). In the present study, we report that while all three LRPs interact strongly with the GGAs via their C-terminal DXXLL motifs, only LRP9 interacts with AP-1/AP-2 via this same motif. We also demonstrate that LRP9 and LRP12 have an additional internal ACLL signal within their cytoplasmic tails that also binds GGAs. These findings have implications concerning the identification of potential cargo molecules for these adaptors as well as the specificity and fidelity of GGA-binding motifs.

Results

The LRP9 and LRP12 cytoplasmic tails contain two functional GGA-binding motifs

The AC-LL signal at the carboxy terminus of the LRP3 sequence (Figure 1A) has been shown to interact with GGAs via yeast-2-hybrid analysis (6). Given the similarity between this motif and the motifs within LRP9 and LRP12 (Figure 1A), we examined whether these receptors interact with GGAs using various fusion proteins (Figure 1B) in GST-pulldown assays. As shown in Figure 2A, GGA1(1-323) with an N-terminal Myc-tag (Myc-GGA1), full-length GGA2 with a C-terminal HA-tag (HA-GGA2), and GGA3(1-241) with an N-terminal Myc-tag (Myc-GGA3) all bound to GST fusions encoding the C-terminal tails of LRP3, 9 and 12, as well as to GST-CI-MPR 18mer that served a positive control. Truncated forms of GGA1 and GGA3 were used because of poor binding exhibited by the full-length proteins due to autoinhibition (7). No binding or only trace binding to GST was observed under these conditions. In reciprocal experiments, we performed GST pull-downs with the VHS domain of GGA2 using cell lysates over-expressing HA-tagged LRP3 and LRP9. In this assay, both molecules bound strongly to GST-GGA2 VHS (Figure 2B, lanes 1 & 3). Truncation of the C-terminal AC-LL signal of LRP3 (HA-LRP3 761 stop) resulted in loss of GGA-binding, consistent with an essential role for this motif in GGA interaction (Figure 2B, lane 2) (6). Surprisingly, however, the truncated LRP9 (HA-LRP9 701 stop) lacking the distal AC-LL signal also strongly bound GST-GGA2 VHS (Figure 2B, lane 4), indicating the presence of a second GGA binding motif.

Inspection of the cytoplasmic tail of LRP9 shows the presence of an internal AC-LL motif that fits the consensus DXXLL sequence recognized by the GGAs (Figure 1A). In a previous study, we established that AP-2 bound to this motif (8). The finding with the HA-LRP9 701 stop construct suggested that this internal AC-LL signal might also bind GGAs. Accordingly, we tested HA-LRP9 685 stop lacking both the proximal and distal AC-LL signals and found that it failed to bind GST-GGA2 VHS (Figure 2B, lane 5). We next performed binding assays using GST fusions encoding the proximal and/or distal AC-LL signals of LRP9. Both motifs, together or alone, bound HA-GGA2 while mutation of the two motifs simultaneously reduced binding to background (GST) levels (Figure 2C, lanes 1-5). Importantly, when the distal AC-LL signal was mutated (LRP9 30mer, distal LL→AA), the fusion peptide mostly retained the ability to bind HA-GGA2 (Figure 2C, lane 3). This clearly demonstrates that the internal AC-LL signal of LRP9 is functional *in vitro*. In contrast, the addition of four alanines to the CI-MPR C-terminal AC-LL signal strongly inhibited GGA binding, while a simultaneous mutation of the ⁻⁴serine (relative to the first leucine) to an aspartate partially overcame this inhibition (Figure 2D, lanes 1-3) (2, 3). Similarly, addition of four alanines to the C-terminal AC-LL signal of LRP3 also greatly

diminished GGA binding (Figure 2D, compare lanes 4 and 5). Based on these findings, we next asked if alanine residues C-terminal to the internal AC-LL signal of LRP9 could perturb its interaction with GGAs. As shown on the left panel of Figure 2E (lanes 2-5), binding of both GST-LRP9 proximal 17mer-LPL→AAA and GST-LRP9 distal 17mer-AAA to HA-GGA2 was significantly reduced. This result suggests that the occurrence of several alanine residues downstream of the AC-LL signal rather than displacement of the latter one to two amino acids from the carboxy terminus is detrimental to the binding of VHS domains. At the same time, the leucine pair cannot occupy the extreme carboxy terminus, as demonstrated for the CIMPR DXXLL motif (2). In the case of the drosophila protein LERP (lysosomal enzyme receptor protein), the leucine pair of the AC-LL signal represent the last two amino acids of the protein. LERP with a C-terminal HA-tag was previously shown to sort cathepsin D and cathepsin L in CI-MPR^{-/-} fibroblasts (9). In order to determine if this C-terminal HA-tag in fact facilitated the interaction of LERP with GGAs, we tested the binding of LERP with either an internal or the C-terminal HA-tag to GST-GGA2 VHS. As shown in Figure 2E, right panel, LERP with the C-terminal HA-tag displayed robust binding to GST-GGA2 VHS while the internally tagged protein with its native terminating leucine pair bound rather poorly, in agreement with the ability of the former to efficiently sort lysosomal enzymes via the GGA pathway (9).

Analysis of the sequence of the cytosolic tail of LRP3 (Figure 1A) reveals only a single GGA-binding DXXLL motif located at the extreme carboxy terminus of the protein, in agreement with the binding data (Figure 2B). However, an additional DXXLL-type motif (Figure 1A) occurs internally within the LRP12 cytosolic tail. In order to assess if this proximal ⁷⁵²DVEML⁷⁵⁶ sequence of LRP12 can bind to GGAs, pull-down experiments were performed by incubating GST-GGA2 VHS with HEK 293 cell lysates expressing either wt HA-LRP12, HA-LRP12 with a distal LL→AA mutation, or HA-LRP12 with combined distal LL→AA/proximal ML→AA mutations (Figure 2F). The results demonstrate that binding of LRP12 to the GGA2 VHS domain is abrogated only when both the distal and proximal AC-LL signals are simultaneously mutated (Figure 2E, lane 5), indicating that at least *in vitro*, the LRP12 internal DVEML sequence is a bona fide GGA-interacting motif. Together, these results indicate that although most GGA-binding DXXLL motifs are found at the carboxy termini of proteins, they can also occur and function at internal sites, depending on the surrounding residues.

The AC-LL motifs of LRP9 but not LRP3 and LRP12 bind to AP-1 and AP-2

In a previous study, we established that GST fusion proteins comprising the proximal (LRP9 p17mer) or distal (LRP9 d17mer) AC-LL signals of LRP9 bound equally well to the AP-2 $\alpha/\sigma 2$ hemicomplex but only the distal signal bound to the AP-1 $\gamma/\sigma 1$ hemicomplex (8). Binding of the distal signal to AP-1 was dependent to a large extent on the glutamate at the -4 position (relative to the first leucine) since substitution with an aspartate at that position greatly impaired this interaction. However, the ⁻⁴glutamate to aspartate substitution had minimal effect on AP-2 binding.

Surprisingly, neither GST-LRP3 16mer nor GST-LRP12 d17mer displayed any appreciable binding to the AP-2 $\alpha/\sigma 2$ hemicomplex or the AP-1 $\gamma/\sigma 1$ hemicomplex (Figure 3A). As expected, the LRP9 d17mer bound strongly to both hemicomplexes. The LRP3 and LRP12 sequences differ from the LRP9 sequence in having an aspartate at the -4 position. However, the fact that LRP9 d17mer retains AP-2 binding following a ⁻⁴glutamate to aspartate substitution suggests that there must be other residues that are lacking or perhaps inhibiting the interaction of LRP3 and LRP12 with AP-2. An analysis of various AP-1/AP-2 interacting AC-LL signals from a number of proteins reveals that the amino acid proline is the predominant residue present at the -1 position (relative to the first leucine) (1). Mutation of the ⁻¹aspartate to proline within the CI-MPR GGA-binding AC-LL signal, when coupled

with the requisite ⁻⁴serine to glutamate substitution (Figure 1B, GST-CI-MPR 18mer-S→E/ D→P), allowed binding of this GST-peptide fusion to both AP-1 and AP-2 hemicomplexes (Figure 3B, lane 5). Mutation of the CI-MPR ⁻⁴serine to glutamate by itself (Figure 1B) was without effect even though it conformed to the consensus EXXXLL sequence (data not shown). Likewise, mutation of the ⁻¹proline within GST-LRP9 d17mer to an alanine (GST-LRP9 d17mer- A→P) abrogated binding to both hemicomplexes. These results emphasize the importance of a proline residue at the -1 position within the context of certain AP-1/AP-2 interacting AC-LL signals. The GST-LRP3 16mer and GST-LRP12 d17mer constructs, instead, present an alanine at this position (Figure 1B). Thus, we mutated the ⁻¹alanine to a proline together with the ⁻⁴aspartate to glutamate substitution within GSTLRP12 d17mer and performed binding assays with the AP-1 and AP-2 hemicomplexes. As shown in Figure 3B, lane 7, these changes were not sufficient to confer binding of GST-LRP12 d17mer to either hemicomplex even though its core EDEPLL sequence was identical to that of GST-LRP9 d17mer. This result indicates that there may be some other strongly inhibitory residue/s outside of the core motif within the GST-LRP12 d17mer peptide sequence that precludes association with the AP-1 and AP-2 hemicomplexes.

The AC-LL motifs of LRP9 are required for internalization at the plasma membrane

In order to establish that the GST pull-down assays reflected interactions that occurred in intact cells, we analyzed the trafficking of wild-type and mutant forms of LRP9 expressed in CHO cells. An examination of the 248 amino acid cytosolic tail of mouse LRP9 revealed the presence of only three potential sorting signals; the proximal and distal AC-LL signals and a tyrosine-based ⁴⁹⁷YGQL⁵⁰⁰ motif (Figure 1A). Since we have previously reported that a glycine at position 2 of the YXX ϕ motif acts as an inhibitory residue (10), we reasoned that internalization of LRP9 at the plasma was likely to involve interaction of the AC-LL signals with AP-2.

In initial experiments, full-length wild-type protein (LRP9 wt) and mutants lacking either the distal AC-LL signal (LRP9 701 stop) or both the distal and proximal AC-LL signals (LRP9 685 stop), or the full-length protein with both dileucine motifs mutated (LRP9 p/d LL→AA) (Figure 1C) were stably expressed in Chinese hamster ovary (CHO cells). The proteins contained an N-terminal HA-tag for detection.

Immunofluorescence microscopy showed that wild-type LRP9 has a similar intracellular distribution as endogenous CI-MPR, which has been reported to be localized to the TGN and late endosomes in CHO cells (Figure 4) (11). The LRP9 701 stop mutant had a similar localization (Figure 4). LRP9 685 stop and LRP9 p/d LL→AA, on the other hand, displayed increased cell surface distribution with some internal staining (Figure 4). Furthermore, transient expression of LRP9 with either proximal LL→AA or distal LL→AA mutations, either individually or in combination with the YGQL→AGQA mutation, showed a distribution indistinguishable from the wild-type (not shown). These results indicate that either AC-LL motif is sufficient for the localization of LRP9 to the TGN/endosomal system but eliminating both motifs results in a marked redistribution of the protein to the plasma membrane.

Since wild-type LRP9 is intracellular while the double dileucine mutant displays strong cell surface localization, it is possible that LRP9 cycles between the TGN and endosomes via the plasma membrane. Simultaneous mutation or deletion of the proximal and distal dileucine motifs within the LRP9 cytoplasmic tail renders the protein incapable of interacting with both GGAs and AP-1/AP-2. Hence, the redistribution of LRP9 685 stop and LRP9 p/d LL→AA to the plasma membrane could be due to a failure to endocytose properly, as a result of the likely inability to interact with AP-2. Alternately, LRP9 never traffics to the plasma membrane and the increased surface distribution observed with the double dileucine

mutants is the consequence of default transport to the cell surface due to loss of GGA-binding. To distinguish between these two possibilities, point mutations were generated in the LRP9 cytoplasmic tail that selectively affects only GGA ($^{-3}\text{D}\rightarrow\text{A}$) or AP-1/AP-2 ($^{-4}\text{E}\rightarrow\text{A}$) binding. Pull-down assays with GST-LRP9 d17mer harboring either the $^{-3}\text{D}\rightarrow\text{A}$ or $^{-4}\text{E}\rightarrow\text{A}$ mutations confirmed the requirement for an aspartate at the -3 position for GGA binding and a glutamate at the -4 position for AP-1/AP-2 binding (Figure 5A).

We next examined the effects of the distal $^{-3}\text{D}\rightarrow\text{A}$ and $^{-4}\text{E}\rightarrow\text{A}$ mutations on the distribution of LRP9 within a cell in the context of the protein with the proximal LL \rightarrow AA mutation in order to rule out any contribution from the proximal AC-LL signal. Indirect immunofluorescence microscopy of nonpermeabilized CHO cells stably expressing either LRP9 wt or LRP9 685 stop indicates strong surface expression only with the truncation mutant lacking both AC-LL signals (Figure 5B, left panel). Since almost every cell expressing LRP9 685 stop but not LRP9 wt gave a clear positive signal under these circumstances, CHO cells transiently transfected with either LRP9 pLL \rightarrow AA/dD \rightarrow A or LRP9 pLL \rightarrow AA/dE \rightarrow A were similarly subject to immunofluorescence microscopy using intact cells. Very little surface immunofluorescence beyond background level was observed with the non-permeabilized CHO cells transiently expressing LRP9 pLL \rightarrow AA/dD \rightarrow A (Figure 5B, left panel). Detergent-permeabilized cells expressing this mutant, however, clearly displayed an intracellular distribution of the protein, demonstrating that the transfection was successful (Figure 5B, right panel). Transient expression of LRP9 pLL \rightarrow AA/dE \rightarrow A, meanwhile, gave very similar results to the LRP9 685 stop mutant under non-permeabilizing conditions (Figure 5B, left panel), indicating that GGA-binding alone is not sufficient to retain LRP9 within the cell and that the normal trafficking itinerary of the protein likely involves transit to the plasma membrane and internalization via the AP-2 dependent pathway.

As a means to confirm the qualitative immunofluorescence data, we performed cell-surface biotinylation and streptavidin-agarose pull-downs to determine the percentage of receptor at the cell surface. Initial experiments were performed using CHO cells stably expressing either wild-type or the LRP9 701 stop and LRP9 685 stop mutants. Consistent with the immunofluorescence data, only LRP9 685 stop showed a significant increase in cell-surface expression (Figure 5C, left panel, compare PD signal of wt, 701 stop and 685 stop). Although we observed only approximately 20% of LRP9 685 stop at the cell surface by this method (Figure 5C, right panel), we surmise this is an underestimate of the total amount possibly due to inefficient tagging of this mutant at the cell surface by biotinylation, as previously reported for a number of other proteins (12, 13). Additional mutants transiently expressed in CHO cells and quantitated the same way reveal that only the double dileucine mutant of LRP9 (LRP9p/d LL \rightarrow AA) shows significantly elevated cell-surface expression similar to LRP9 685 stop (Figure 5D).

Rapid internalization of LRP9 requires only one AC-LL motif

Since the LRP9 double dileucine mutant was redistributed to the plasma membrane, we reasoned that the wild-type receptor may undergo rapid endocytosis from the cell surface via the dileucine motifs. To investigate this, an HA-tagged chimeric receptor consisting of the fourth ligand binding and transmembrane domains of LRP1 (herein referred to as mini-receptor LRP4 or mLRP4) and the entire 248 amino acid cytosolic tail of LRP9 was constructed to facilitate the measurement of the endocytic rate conferred by the LRP9 tail after transient transfection into CHO cells (14). The mLRP4-LRP9 tail chimeric construct was necessitated by the fact that very poor binding of iodinated anti-HA antibody to the extracellular domain of LRP9 was observed irrespective of its cytosolic tail, and we attribute this to a masking effect of the HA-epitope within the native protein in the endocytosis assays. When internalization of the wild-type receptor tail chimera was measured by this

method using iodinated anti-HA, it was found to internalize with a half-time ($t_{1/2}$) of approximately four minutes (Figure 6A), similar to the rate displayed by the LDL receptor but slower than mLRP4 with its native cytosolic tail (14). The mutant of mLRP4 without a cytosolic tail (mLRP4 tailless) internalized very slowly (less than 10%) in the same time period (Figure 6A). The proximal LL→AA mutation within the LRP9 tail did not change the rate of endocytosis of the chimera, while the distal LL→AA mutation only slightly decreased the rate (Figure 6B). Mutation of both the proximal and distal dileucines (LRP9p/d LL→AA), however, decreased the endocytosis rate to that of mLRP4 tailless (Figure 6B).

We next tested the rate of endocytosis of an mLRP4-LRP9 chimeric protein with the two proximal aspartates (^{-3}D - ^{-2}D) together with the distal dileucines mutated to alanines (Figure 1C, LRP9 pDD→AA/dLL→AA). The ^{-2}D →A change was necessary since the proximal AC-LL signal presented an additional alanine at the +2 position (relative to the first leucine, see Figure 1A). Hence, this chimeric mutant would not be expected to interact with GGAs but should bind AP-2 and endocytose normally. As shown in Figure 5C, mLRP4-LRP9 pDD→AA/dLL→AA internalized at almost the same rate as mLRP4-LRP9 dLL→AA. However, mutation of the entire proximal acidic cluster together with the distal dileucines (Figure 1C, LRP9 pAC/dLL→AA), which should preclude AP-2 binding, reduced the rate of endocytosis of this chimeric mutant (mLRP4-LRP9 pAC/dLL→AA) to that of mLRP4 tailless (Figure 6D). These results provide further evidence that endocytosis mediated by the LRP9 tail is via the AP-2 dependent pathway.

Figure 6E shows that mutation of the YGQL motif to AGQA had no effect on the rate of endocytosis of the chimeric receptor. In addition, combining this mutation with mutations of either the proximal or distal AC-LL signal did not impair endocytosis (not shown). These findings indicate that the LRP9 YGQL motif is not a functional endocytosis signal, thereby excluding the possibility that rapid internalization requires two of the three potential internalization signals. These data are in agreement with the immunofluorescence and cell-surface biotinylation analyses.

Discussion

These studies of the trafficking signals of LRP9 have revealed several novel aspects of the motifs. The first concerns the distal EDEPLL sequence which serves as a binding partner for both the GGAs and AP-1/AP-2. As far as we are aware, this is the first documented example of this type of overlap. Two other proteins with GGA-binding motifs, BACE (DDISLL) (15) and SorLA (DDVPMV) (16), could potentially bind AP-2. While this has not been experimentally established for BACE, it has been reported that the GGA-binding DDVPMV motif of sorLA is not involved in binding either AP-1 or AP-2. Instead, sorLA probably utilizes an internal EDAPMI motif for binding these two clathrin adaptors and for endocytosis (17).

Although the DDEALL motifs of the related proteins, LRP3 and LRP12, also appear to perfectly fit the consensus sequence for both GGA and AP-2 binding, they only interacted with the former. We have previously demonstrated that amino acids other than the [D,E] and L[LI] in the signature [D,E]XXXL[L,I] sequence can greatly influence whether a particular dileucine-based motif is functional or not in its interaction with AP-1 or AP-2 (8). In the case of the CI-MPR GGA-binding DXXLL motif, mutation of the $^{-4}$ serine to glutamate (SDEDLL→EDEDLL) is insufficient for AP-1 /AP-2 hemicomplex-binding, while a simultaneous mutation of the $^{-1}$ aspartate to proline (SDEDLL→EDEPLL) confers binding to both hemicomplexes. Although proline occurs more frequently than other amino acids in the -1 position of [D,E]XXXL[L,I] signals (1), the significance of this is unclear in the absence of a co-crystal structure of a proline-containing AC-LL peptide bound to the AP-1/

AP-2 hemicomplex. Much to our surprise, analogous changes in the LRP12 distal AC-LL signal (DDEALL→EDEPLL) did not permit binding to either hemicomplex. It is possible that the presence of one or more inhibitory amino acids flanking the core AC-LL signal interfere with the binding. A similar phenomenon was observed with the cation-dependent MPR wherein a naturally-occurring methionine residue C-terminal to the GGA-binding DXXLL motif was responsible for the extremely weak or undetectable binding of this receptor to GGAs (2,6). Taken together, these findings indicate that in some cases, dileucine-based motifs are fine-tuned to achieve a high degree of specificity in their interactions with clathrin adaptors.

Another unexpected finding to emerge from these studies was the presence of a second, internal GGA-binding motif within the cytoplasmic tails of LRP9 and LRP12. It has been shown that GGA1 and GGA3 contain internal dileucine motifs in their hinge domains that are capable of binding their corresponding VHS domains, thereby blocking cargo binding (7). However, with the possible exception of Stabilin1 (18), all GGA-binding motifs within receptor cytoplasmic tails that have been characterized to date are located one or two amino acids from the carboxy-terminus of the proteins (1). In fact, the robust interaction between the CI-MPR tail and GGAs is compromised by addition of two or four alanine residues to the end of the tail sequence or terminating the protein with the dileucine sequence (Figure 2C) (2,3). The co-crystal structures of the GGA1/GGA3 VHS domains with a peptide corresponding to the human CI-MPR AC-LL signal show that in addition to the anchor aspartate and dileucine residues, the C-terminal isoleucine side chain (valine in the case of bovine CI-MPR) that is two amino acids removed from the leucine pair forms a hydrophobic cluster with neighboring amino acids in the VHS domain that could stabilize the peptide-VHS complex (3,19). Furthermore, phosphorylation of the CI-MPR⁻⁴serine introduces electrostatic interactions with 2 basic residues within the GGA VHS domain that is not present in the unphosphorylated state of the receptor tail (20). Also, the C-terminal carboxyl group when spaced one or two amino acids from the dileucine is thought to interact weakly with the VHS domain and contribute to binding in a secondary capacity, in part explaining why most GGA-interacting DXXLL motifs are situated one to two residues from the carboxy terminus (3). Hence, the GGA-binding AC-LL signal was proposed to function as a distinctive motif for specific binding that relies not on a single high-affinity interaction with one bulky side chain as a linchpin, but rather on a distributed set of several weaker interactions with medium-sized chains (3). This idea is borne out by our finding that mutation of the CI-MPR⁻⁴serine to an aspartate, to mimic a phosphorylated serine, is able to partially overcome the inhibitory effects due to addition of four alanines which would negate the contribution of the carboxyl group (Figure 2C). Internal GGA-binding motifs would lack this carboxyl group, making the secondary contribution from the downstream hydrophobic amino acid more critical. The LRP9 and LRP12 internal AC-LL signals possess hydrophobic residues located one and three amino acids downstream of the dileucine sequence. These residues may facilitate the strong interaction with GGAs. Our result with the mutant GST-LRP9 p17mer (proximal LPL→AAA) indicates that this indeed may be the case, that is, the addition of alanines per se and not displacement from the carboxy terminus is what makes for a poor GGA-binding signal. In addition to LRP9 and LRP12, Stabilin1 has also been reported to have an internal GGA-interacting AC-LL signal (DDSLLEED) within its cytosolic tail (18). However, in our hands, it exhibited extremely poor or undetectable binding to the GGA2 VHS domain using the standard GST pull-down assay (not shown). A possible explanation for the conflicting data is that the association of the Stabilin1 AC-LL signal is too weak to be detected using our assay system while in the reported study (18), *in vitro* transcribed-translated and radiolabeled GGAs were used. The occurrence of 3 acidic residues immediately downstream of the DDSLL sequence may in part explain why Stabilin-1 associates so poorly with the GGAs in our binding assay. This is

in agreement with the observation that DXXLL signals cannot terminate with the leucine pair (3).

To date, only 8 membrane proteins have been documented to have motifs that bind to GGAs (including LRP3, LRP9, and LRP12). In view of our finding of high affinity GGA binding motifs in internal locations, it seems possible that GGA-interacting proteins may have been missed by searches that are restricted to the C-terminal region of membrane proteins. It will be interesting to see if a more general search turns up new candidate molecules as being GGA partners.

While these findings represent the first characterization of the cellular trafficking of LRP9, the function of this membrane protein as well as its related molecules, LRP3 and LRP12, remains unknown. A similar distribution of LRP9 with the CI-MPR at the TGN and endosomes, and its association with the GGAs, suggest that LRP9 may play a role in the trafficking of ligands between these intracellular compartments. Our studies further indicate that LRP9 traffics to the cell-surface and undergoes rapid endocytosis, most likely via the AP-2 pathway, raising the possibility that extracellular ligands may also exist. Our present efforts are focused on identifying potential ligands of this putative receptor.

Materials & Methods

Materials

Mouse anti-HA monoclonal antibody was purchased from Covance (Berkeley, CA), while the anti-myc 9E10 monoclonal antibody was from Santa Cruz Biotechnology, Inc. (Santa Cruz, CA). Affinity purified rabbit anti-bovine CIMPR antibody was prepared by Walter Gregory in our laboratory. A cDNA clone encoding human LRP12 was a gift from J. Justin McCormick (Michigan State University, East Lansing, Michigan) while the C-terminally tagged HALERPpCDNA3.1 clone was generously provided by Regina Pohlmann (Universitaets-Klinikum-Muenster, Muenster, Germany). Carrier-free Na¹²⁵I was purchased from PerkinElmer Life and Analytical Sciences (Shelton, CT). PD-10 desalting columns, HRP-conjugated secondary antibodies, and Glutathione-Sepharose 4B were from GE Healthcare (Little Chalfont, Buckinghamshire, United Kingdom), while Streptavidin-agarose was from Sigma (St. Louis, MO). Cellfectin and Alexa 488 and 568-conjugated secondary antibodies were purchased from Invitrogen (Carlsbad, CA). Mirus Trans-IT CHO transfection kit was from Mirus (Madison, WI).

Cell culture and transfection

The LRP1-null Chinese hamster ovary (CHO) cell line (kindly provided by David FitzGerald, National Institutes of Health) was cultured in Ham's F-12 medium as described (21). Transient and stable transfection into CHO-LRP null cells was achieved by transfection of 2 µg of plasmid DNA in 6-well plates using the Mirus Trans-IT CHO kit according to the manufacture's instructions. Endocytosis assays following transient transfection were carried out 24 hours post-transfection and were performed at least three times. Stable transfectants were selected using 700µg/ml G418 and maintained with 350µg/ml G418. Clonal purity was assayed by Western blotting and immunofluorescence analysis using anti-HA IgG. At least two independently derived clones were used for each assay. Sf9 insect cells were cultured at room temperature and atmospheric conditions in Sf-900 II SFM and transfected with Cellfectin, both purchased from Invitrogen, according to the manufacturer's instructions.

Plasmid construction

The mouse LRP9 and LRP12, and human LRP3 clones encoding the complete cDNAs were obtained from American Type Culture Collection. Amino-terminal HA epitopes were inserted several amino acids downstream of the sequence encoding the signal peptide of each LRP as predicted by SignalP (The Center for Biological Sequence Analysis, Technical University of Denmark, Lyngby, Denmark). The chimeric HA-tagged LRP1 domain IV minireceptor (mLRP4) (10) fused to the full-length cytosolic tail of LRP9 used as a reporter for endocytosis assays was created by cloning the LRP9 tail into pcDNA3.1/mLRP4 tailless using standard molecular biology techniques. Mutations in the cytoplasmic tails of the wild-type or chimeric receptor were achieved using the QuikChange site-directed mutagenesis system (Stratagene, La Jolla, CA). LERP with an internal HA epitope was made from HALERPpCDNA3.1 (9) by first introducing a stop codon immediately after the C-terminal leucine (L886) to restore the native carboxy terminus, followed by insertion of the HA sequence downstream of G875 of the LERP cytosolic tail. All constructs (Figure 1C) were sequenced prior to transfection.

Expression/ purification of GST fusion proteins and expression of adaptor subunits in insect cells

All GST fusions (Figure 1B) in pGEX expression vectors were expressed in the *Escherichia coli* strain BL-21 (RIL) (Stratagene) and purified essentially as described previously (22). Expression of GGAs and the AP-1 $\gamma/\sigma 1$ and AP-2 $\alpha/\sigma 2$ hemicomplexes in Sf9 insect cells has been described (2, 7, 8).

Binding assays

The binding of Sf9 cell-expressed adaptor proteins to the various GST fusion proteins was assayed in assay buffer A (25 mM HEPES-KOH pH 7.2, 125 mM potassium acetate, 2.5 mM magnesium acetate, 1 mM DTT, and 0.4% Triton X-100) in a final volume of 300 μ l in 1.5 ml pre-siliconized microcentrifuge tubes (MidSci, St. Louis, MO). Routinely, 200 μ g GST-fusion proteins were first immobilized on 50 μ l of packed glutathione-Sepharose 4B for 2 hours at room temperature. The beads with bound proteins were pelleted by centrifugation at $750 \times g$ for 1 min, the beads were washed once with assay buffer B (buffer A with 0.1% Triton- X-100), and 300 μ l of the Sf9 cell lysate in assay buffer A at a final concentration of 2-5 mg/ml was added to the washed beads. The binding reactions were allowed to proceed for 2 h at 4°C with tumbling, after which the samples were subjected to centrifugation at $750 \times g$ for 1 min. An aliquot of the supernatant was saved, and the pellets were washed four times each by resuspension in 1 ml of cold assay buffer B followed by centrifugation at $750 \times g$. The washed pellets were resuspended in SDS sample buffer and heated at 100°C for 5 min. Unless indicated otherwise, 25% of each pellet and 3% of each supernatant fraction were loaded on SDS PAGE, transferred to nitrocellulose membranes, and probed with anti-HA or anti-Myc antibody. Nitrocellulose membranes were routinely stained with Ponceau solution to ascertain equal loadings of fusion proteins.

Immunofluorescence microscopy

CHO-LRP1 null cells stably expressing wild-type or mutant LRP9s were plated on glass coverslips and fixed in 3.7% formaldehyde in phosphate-buffered saline (PBS) for 15 minutes. Fixed cells were washed with PBS, and blocked and permeabilized with 0.4% Triton X-100, 2% IgG-free bovine serum albumin (BSA) (Jackson ImmunoResearch Laboratories, West Grove, PA) in PBS. Anti-HA mouse mAb (1:1000 dilution) or anti-CI-MPR rabbit polyclonal antibody (1:1000 dilution) were applied in antibody dilution buffer (0.1% Triton X-100, 0.5% IgG-free BSA in PBS) for 1 hr. After washing with PBS, secondary antibodies Alexa 488-anti-mouse and Alexa 568-anti-rabbit (Invitrogen) (1:500

dilution) were applied in antibody dilution buffer for 1hr. The coverslips were washed and mounted on slides with mounting medium (Biomedex, Foster City, CA). Images were obtained with an Olympus IX70 inverted microscope (Olympus, Tokyo, Japan) and processed using Metamorph software (Molecular Devices, Sunnyvale, CA).

Cell-surface biotinylation and kinetic analysis of endocytosis

Cell-surface biotinylation experiments to determine the ratio of cell-surface: total receptor, and endocytosis assays to measure the fraction of internalized chimeric receptors at various time points have been described in detail elsewhere (8,14). The quantitation of the ratio of cell-surface to total biotinylated receptors was performed by probing western blots with ECL plus (GE Healthcare) and scanning with a Typhoon phosphorimager (GE Healthcare). ImageQuant software (GE Healthcare) was used to calculate the density of each band, and these numbers were normalized to the amount of sample loaded. The percent cell surface receptor was calculated by dividing pellet values by total values. The averages of triplicate wells were plotted; error bars represent standard deviation.

For endocytosis assays, the sum of ligand that was internalized plus that which remained on the cell surface after each assay was used as the maximum potential internalization. The fraction of internalized ligand after each time point was calculated and plotted.

Acknowledgments


This work was supported by National Institutes of Health grants RO1 CA-08759 to S. K. and RO1 AG-027924 to G. B.

References

1. Bonifacino JS, Traub LM. Signals for sorting of transmembrane proteins to endosomes and lysosomes. *Annu Rev Biochem.* 2003; 72:395–447. [PubMed: 12651740]
2. Doray B, Bruns K, Ghosh P, Kornfeld SA. Interaction of the cation-dependent mannose 6-phosphate receptor with GGA proteins. *J Biol Chem.* 2002; 277:18477–18482. [PubMed: 11886874]
3. Misra S, Puertollano R, Kato Y, Bonifacino JS, Hurley JH. Structural basis for acidic-cluster-dileucine sorting-signal recognition by VHS domains. *Nature.* 2002; 415:933–937. [PubMed: 11859375]
4. Sugiyama T, Kumagai H, Morikawa Y, Wada Y, Sugiyama A, Yasuda K, Yokoi N, Tamura S, Kojima T, Nosaka T, Senba E, Kimura S, Kadowaki T, Kodama T, Kitamura T. A novel low-density lipoprotein receptor-related protein mediating cellular uptake of apolipoprotein E-enriched beta-VLDL in vitro. *Biochemistry.* 2000; 39:15817–15825. [PubMed: 11123907]
5. Battle MA, Maher VM, McCormick JJ. ST7 is a novel low-density lipoprotein receptor-related protein (LRP) with a cytoplasmic tail that interacts with proteins related to signal transduction pathways. *Biochemistry.* 2003; 42:7270–7282. [PubMed: 12809483]
6. Takatsu H, Katoh Y, Shiba Y, Nakayama K. Golgi-localizing, gamma-adaptin ear homology domain, ADP-ribosylation factor-binding (GGA) proteins interact with acidic dileucine sequences within the cytoplasmic domains of sorting receptors through their Vps27p/Hrs/STAM (VHS) domains. *J Biol Chem.* 2001; 276:28541–28545. [PubMed: 11390366]
7. Doray B, Bruns K, Ghosh P, Kornfeld S. Autoinhibition of the ligand-binding site of GGA1/3 VHS domains by an internal acidic cluster-dileucine motif. *Proc Natl Acad Sci U S A.* 2002; 99:8072–8077. [PubMed: 12060753]
8. Doray B, Lee I, Knisely J, Bu G, Kornfeld S. The $\gamma/\sigma 1$ and $\alpha/\sigma 2$ hemicomplexes of clathrin adaptors AP-1 and AP-2 harbor the dileucine recognition site. *Mol Biol Cell.* 2007; 18:1887–1896. [PubMed: 17360967]
9. Dennes A, Cromme C, Suresh K, Kumar NS, Eble JA, Hahnenkamp A, Pohlmann R. The novel *Drosophila* lysosomal enzyme receptor protein mediates lysosomal sorting in mammalian cells and

- binds mammalian and *Drosophila* GGA adaptors. *J Biol Chem.* 2005; 280:12849–12857. [PubMed: 15664992]
10. Jadot M, Canfield WM, Gregory W, Kornfeld S. Characterization of the signal for rapid internalization of the bovine mannose 6-phosphate/insulin-like growth factor-II receptor. *J Biol Chem.* 1992; 267:11069–11077. [PubMed: 1317852]
 11. Lin SX, Mallet WG, Huang AY, Maxfield FR. Endocytosed cation-independent mannose 6-phosphate receptor traffics via the endocytic recycling compartment en route to the trans-Golgi network and a subpopulation of late endosomes. *Mol Biol Cell.* 2004; 15:721–733. [PubMed: 14595110]
 12. Zhang X, Arvan P. Cell type-dependent differences in thyroid peroxidase cell surface expression. *J Biol Chem.* 2000; 275:31946–31953. [PubMed: 10924504]
 13. Gottardi CJ, Dunbar LA, Caplan MJ. Biotinylation and assessment of membrane polarity: caveats and methodological concerns. *Am J Physiol.* 1995; 268:F285–F295. [PubMed: 7864168]
 14. Li Y, Lu W, Marzolo MP, Bu G. Differential functions of members of the low density lipoprotein receptor family suggested by their distinct endocytosis rates. *J Biol Chem.* 2001; 276:18000–18006. [PubMed: 11279214]
 15. He X, Chang WP, Koelsch G, Tang J. Memapsin 2 (beta-secretase) cytosolic domain binds to the VHS domains of GGA1 and GGA2: implications on the endocytosis mechanism of memapsin 2. *FEBS Lett.* 2002; 524:183–187. [PubMed: 12135764]
 16. Jacobsen L, Madsen P, Nielsen MS, Geraerts WPM, Gliemann J, Smit AB, Petersen CM. The sorLA cytoplasmic domain interacts with GGA1 and -2 and defines minimum requirements for GGA binding. *FEBS Lett.* 2002; 511:155–158. [PubMed: 11821067]
 17. Nielsen MS, Gustafsen C, Madsen P, Nyengaard JR, Hermey G, Bakke O, Mari M, Schu P, Pohlmann R, Dennes A, Petersen CM. Sorting by the cytoplasmic domain of the amyloid precursor protein binding receptor SorLA. *Mol Cell Biol.* 2007; 19:6842–6851. [PubMed: 17646382]
 18. Kzhyshkowska J, Gratchev A, Martens JH, Pervushina O, Mamidi S, Johansson S, Schledzewski K, Hansen B, He X, Tang J, Nakayama K, Goerdts S. Stabilin-1 localizes to endosomes and the trans-Golgi network in human macrophages and interacts with GGA adaptors. *J Leukoc Biol.* 2004; 76:1151–1161. [PubMed: 15345724]
 19. Shiba T, Takatsu H, Nogi T, Matsugaki N, Kawasaki M, Igarashi N, Suzuki M, Kato R, Earnest T, Nakayama K, Wakatsuki S. Structural basis for recognition of acidic-cluster dileucine sequence by GGA1. *Nature.* 2002; 415:937–941. [PubMed: 11859376]
 20. Kato Y, Misra S, Puertollano R, Hurley JH, Bonifacino JS. Phosphoregulation of sorting signal-VHS domain interactions by a direct electrostatic mechanism. *Nature Struct Biol.* 2002; 9:532–536. [PubMed: 12032548]
 21. FitzGerald DJ, Fryling CM, Zdanovsky A, Saelinger CB, Kounnas M, Winkles JA, Strickland D, Leppla S. *Pseudomonas* exotoxin-mediated selection yields cells with altered expression of low-density lipoprotein receptor-related protein. *J Cell Biol.* 1995; 129:1533–1541. [PubMed: 7790352]
 22. Doray B, Kornfeld S. γ subunit of the AP-1 adaptor complex binds clathrin: implications for cooperative binding in clathrin vesicle assembly. *Mol Biol Cell.* 2001; 12:1925–1935. [PubMed: 11451993]

A

LRP3 ⁵²¹KLYSLRTQEYRAFETQMRLEAEFVRREAPPSYYGQLIAQGL⁵⁶¹-
 --//-----⁷⁶⁰EASDDEALLVC⁷⁷⁰

LRP9 ⁴⁶⁶KLYAIRTQEYSIFAPLSRMEAEIVQQQAPPSYYGQLIAQGA⁵⁰⁵--
 --//-----⁶⁸²VLSPEDDDVLLLPLAEPEVWVVEAEDEPLLA⁷¹³

LRP12 ⁴⁶⁶KLYAIRTQEYSIFAPLSRMEAEIVQQQAPPSYYGQLIAQGA⁵⁰⁵--
 --//---⁷⁴⁵SGREDDDVEMLIPVS⁷⁶⁰--//---⁸²⁹ETSDDEALLLC⁸³⁹

B

GST-peptides

mLRP9 30mer	SPEDEDDVLLLPLAEPEVWVVEAEDEPLLA
mLRP9 30mer-proxLL→AA	SPEDEDDVAAALPLAEPEVWVVEAEDEPLLA
mLRP9 30mer-disLL→AA	SPEDEDDVLLLPLAEPEVWVVEAEDEPAAA
mLRP9 30mer-p/dLL→AA	SPEDEDDVAAALPLAEPEVWVVEAEDEPAAA
mLRP9 p17mer	SPEDEDDVLLLPLAEPE
mLRP9 p17mer-LPL→AAA	SPEDEDDVLLAAAAEPE
mLRP9 d17mer	AEPEVWVVEAEDEPLLA
mLRP9 d17mer-AAA	AEPEVWVVEAEDEPLLA ^{AAA}
mLRP9 d17mer-D→A	AEPEVWVVEAEAEPLLA
mLRP9 d17mer-E→A	AEPEVWVVEAAEPLLA
mLRP9 d17mer-P→A	AEPEVWVVEAEDEALLA
hLRP3 16mer	CSPMLEASDDEALLVC
hLRP3 16mer-AAAA	CSPMLEASDDEALLVCAAAA
hLRP12 d17mer	EVTLNKNETSDDEALLLC
hLRP12 d17mer-D→E/A→P	EVTLNKNETSEDEPLLLC
bCI-MPR 18mer	ATPISTFHDDSDEDLLHV
bCI-MPR 18mer-AAAA	ATPISTFHDDSDEDLLHVAAAA
bCI-MPR 18mer-AAAA/S→D	ATPISTFHDDDDDEDLLHVAAAA
bCI-MPR 18mer-S→E	ATPISTFHDDDEDEDLLHV
bCI-MPR 18mer-S→E/D→P	ATPISTFHDDDEDEPLLLHV



Figure 1. The cytosolic tails of LRP9 and LRP12 contain 2 AC-LL signals

(A) The partial amino acid sequences of the cytosolic tails of LR3, LRP9 and LRP12 are shown from the end of the transmembrane (TM) segments to the C-termini of the proteins. (B) Sequences of the various AC-LL signals used in this study. Proteins were expressed as GST-fusions and purified from *E. coli* BL21 cells. (C) Schematic representation of wild-type and mutant LRP9 and LRP12 constructs used in the immunofluorescence and cell-surface biotinylation studies. For endocytosis assays, mLRP4-LRP9 chimeric constructs were made by fusing the fourth ligand binding and transmembrane domains of LRP1 with the wild type or mutant cytosolic tails of LRP9.

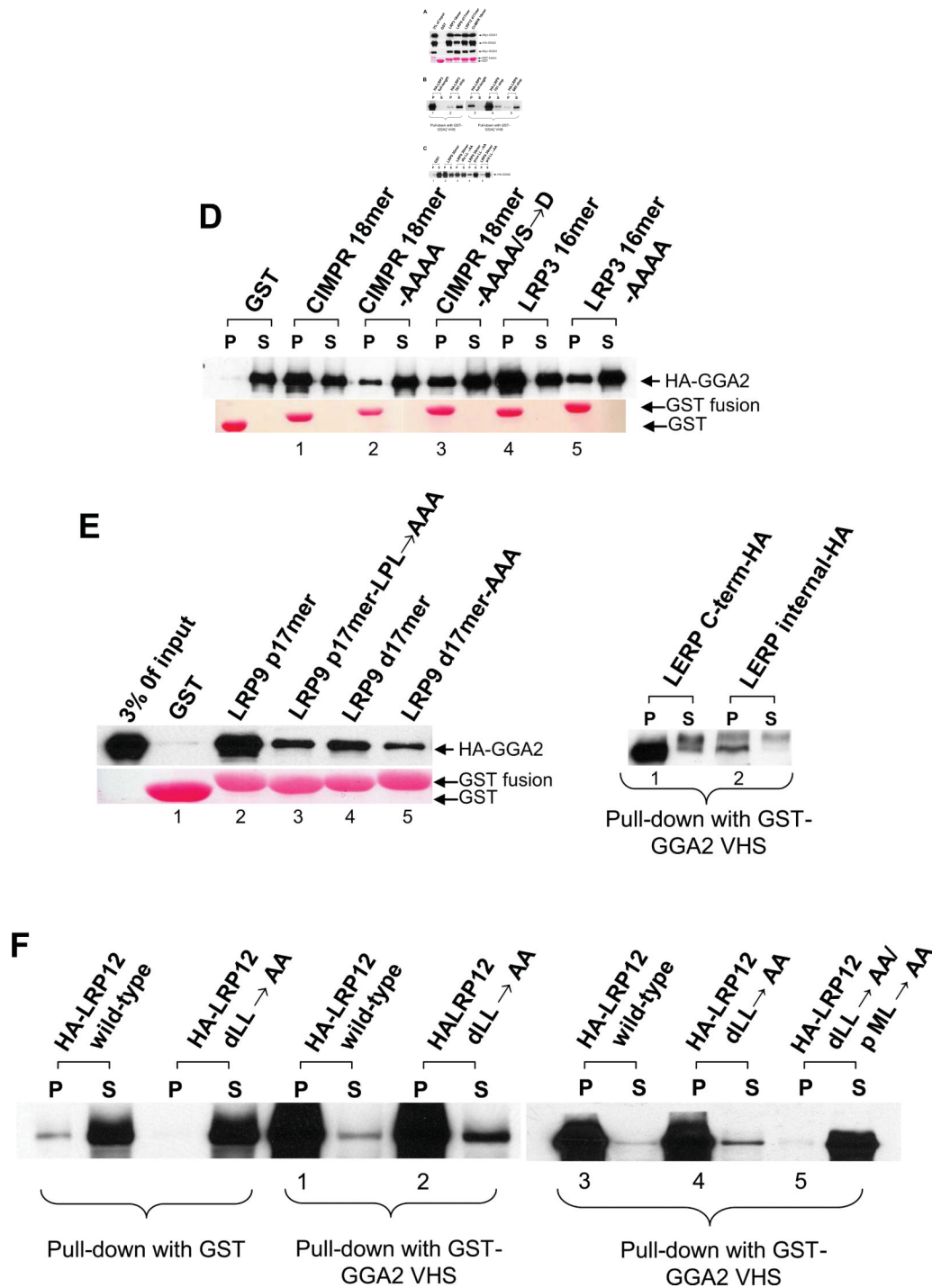


Figure 2. LRP9 and LRP12 contain an internal GGA binding sequence in addition to a carboxy-terminal DXXLL motif

(A-F) Pull down assays were performed using GST fusions encoding the indicated AC-LL signals of the different LRPs with Sf9 cell-expressed GGAs (A, C, D, and E-left panel), or GST-GGA2 VHS with HEK 293 cell-expressed wild-type and mutant LRPs and LERP (B, E-right panel, and F). Ponceau staining of the membrane (A, D, and E-left panel) indicates that similar amounts of the various GST-fusions were used.

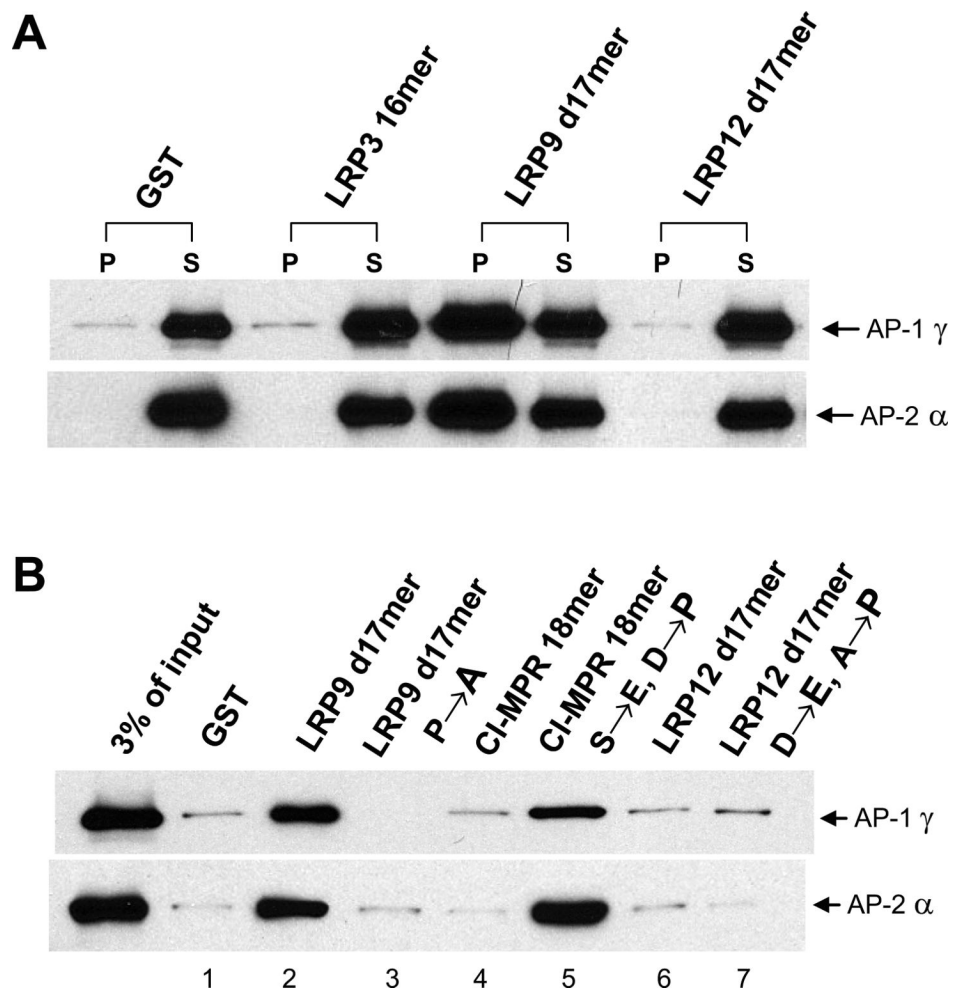


Figure 3. Only the LRP9 distal AC-LL signal binds to both the AP-1 and AP-2 hemicomplexes (A and B) The AP-1 $\gamma/\sigma 1$ and AP-2 $\tilde{\alpha}/\sigma 2$ hemicomplexes were expressed in Sf9 insect cells and served as the source of adaptor protein in pull-down assays for binding to the various GST fusions encoding the indicated ACLL signals of the different LRPs. (B) The binding assays were performed as in (A) with the wild type and mutant CI-MPR and LRP12 cytosolic tails fused to GST.

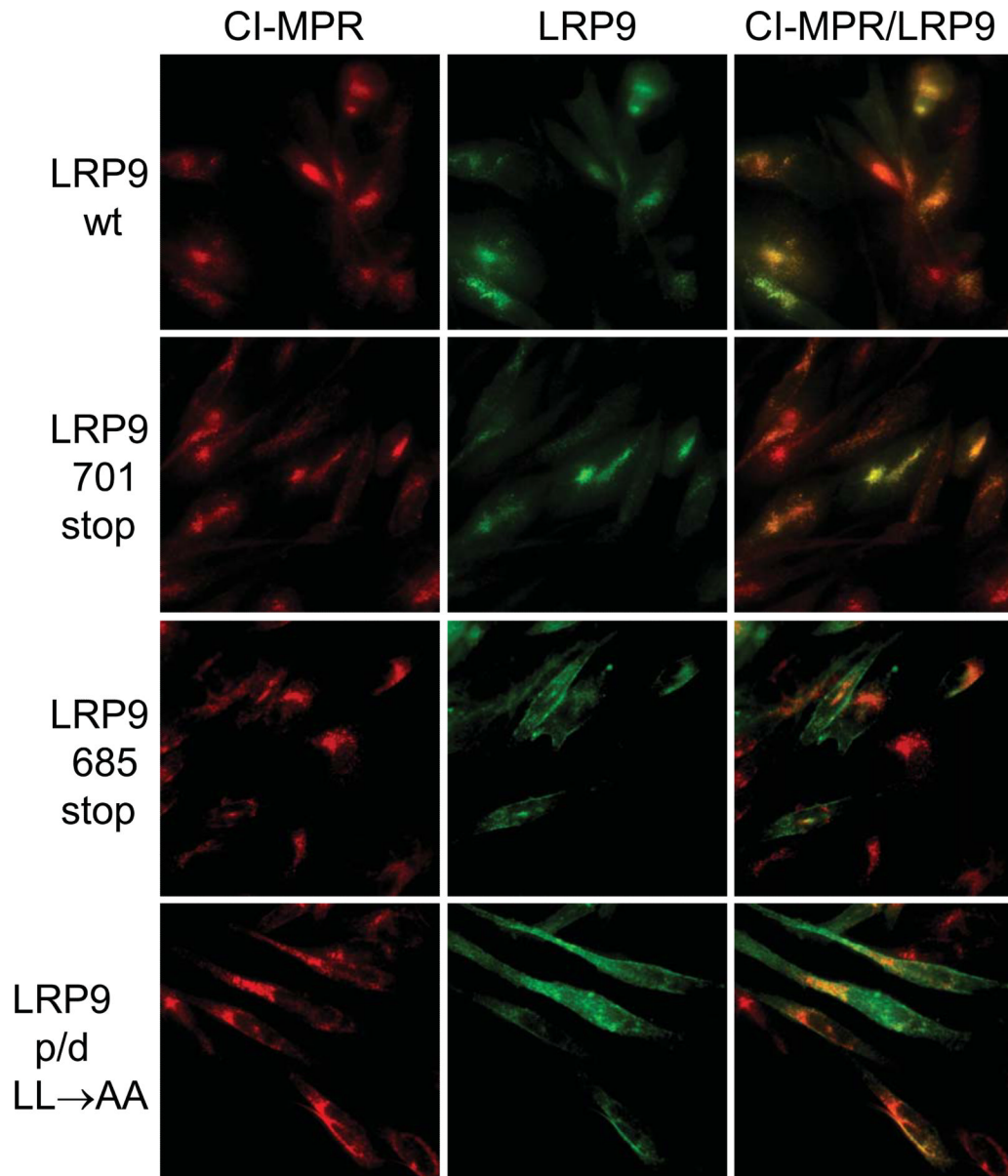
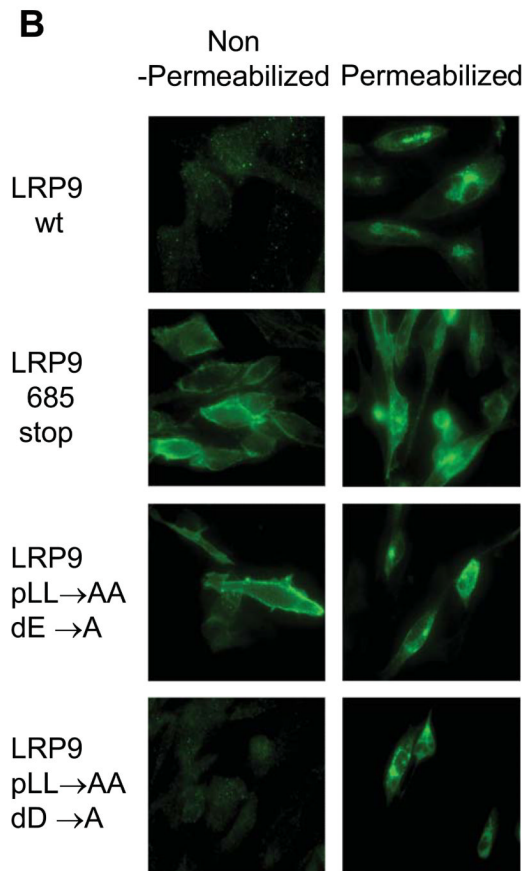
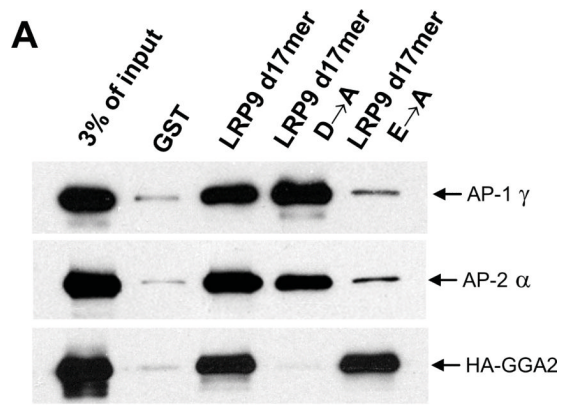


Figure 4. Either AC-LL signal of LRP9 is sufficient for the intracellular localization of the protein

Immunofluorescence microscopy of fixed and permeabilized CHO cells stably expressing wild-type or mutant LRP9 (green) and endogenous CI-MPR (red). Colocalization is observed by merging the green and red signals.



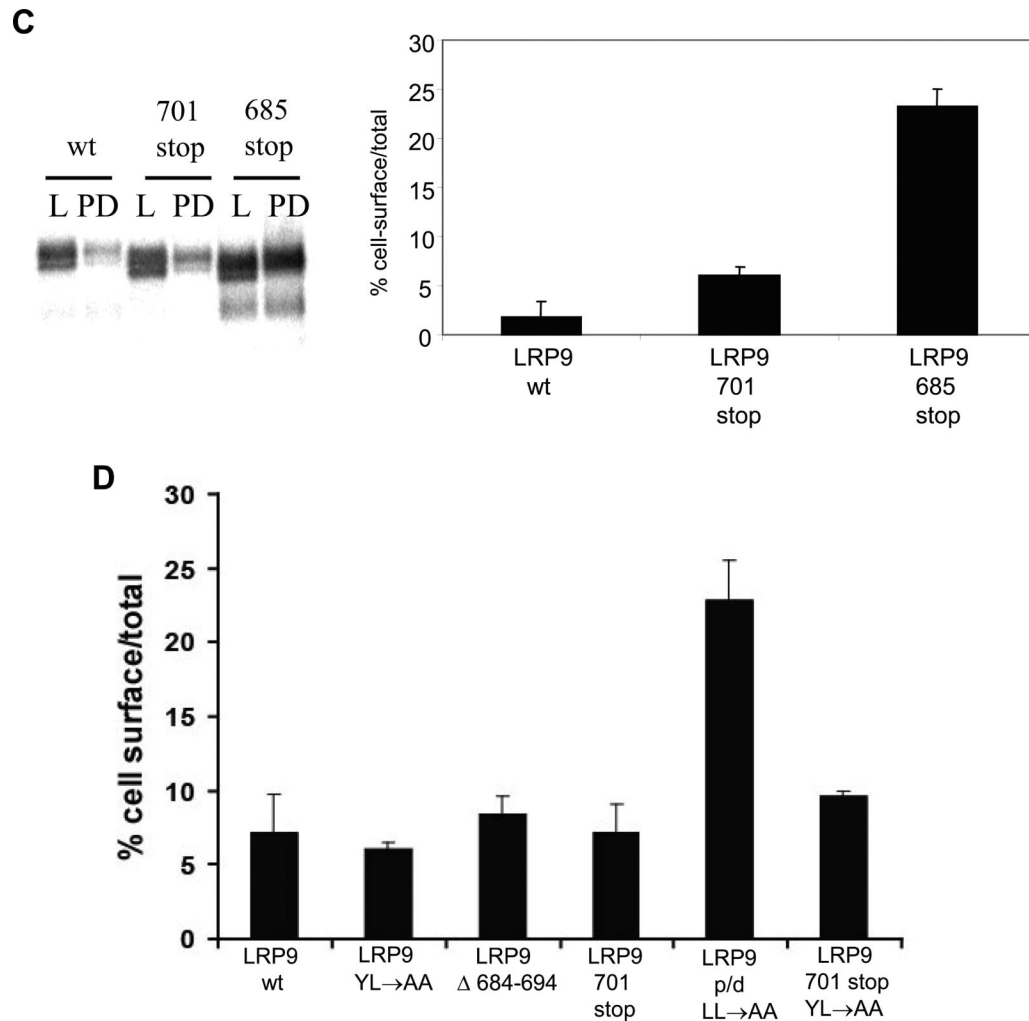


Figure 5. Distinct requirements for the -3 aspartate and -4 glutamate of the distal AC-LL signal for the trafficking of LRP9

(A) Binding assays were performed with the D→A and E→A mutants of GST-LRP9 d17mer to ascertain the distinct requirement for the ⁻³D and ⁻⁴E for GGA versus AP-1/AP-2 binding, respectively. (B) Immunofluorescence analysis was performed using non-permeabilized or permeabilized CHO cells either stably expressing wild-type LRP9 (LRP9 wt) and the truncation mutant lacking both AC-LL signals (LRP9 685 stop), or transiently expressing the LRP9 pLL→AA/dD→A and LRP9 pLL→AA/dE→A mutants. (C) Cell-surface biotinylation was performed as described under Materials & Methods with the indicated stable cell lines to determine the ratio of cell-surface to total biotinylated receptors by probing western blots (left panel) and scanning with a phosphorimager to quantitate the values (right panel). 20% of the total cell lysate (L) and 50% of the streptavidinagarose pull-down sample (PD) were loaded. (D) Cell-surface biotinylation and quantitation were performed in the same manner except all proteins were transiently expressed in CHO cells.

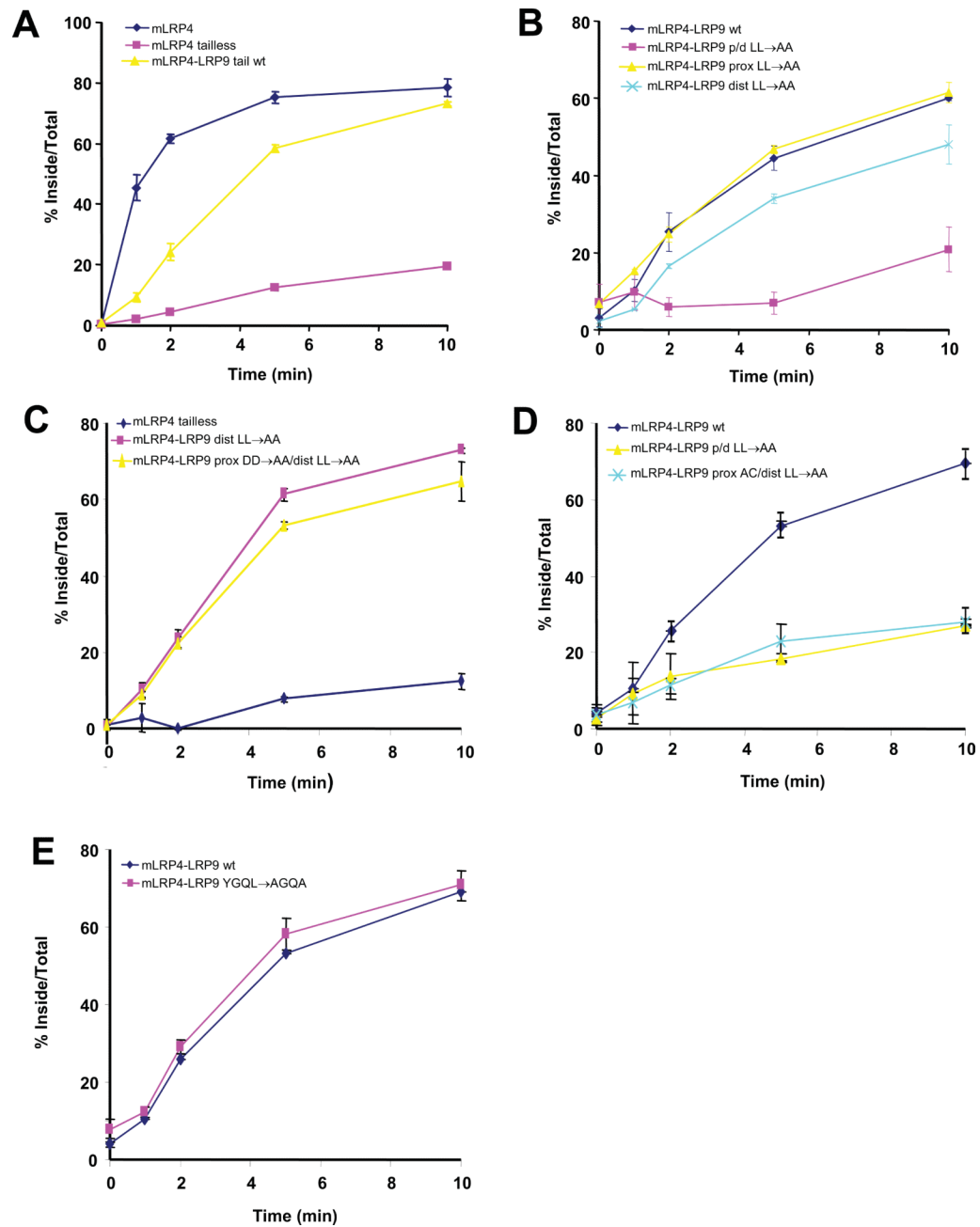


Figure 6. Rapid internalization of LRP9 requires either one of the two AC-LL signals but not the YGQL motif

(A-E) Kinetic analysis of endocytosis with CHO cells transiently transfected with the indicated constructs was performed 24hrs post-transfection. The sum of ligand that was internalized plus that which remained on the cell surface after each assay was used as the maximum potential internalization. The fraction of internalized ligand after each time point was calculated and plotted.